HHS Public Access

Author manuscript

Mucosal Immunol. Author manuscript; available in PMC 2016 May 01.

Published in final edited form as:

Mucosal Immunol. 2015 November ; 8(6): 1313–1323. doi:10.1038/mi.2015.21.

The prostaglandin D_2 receptor CRTH2 regulates accumulation of group 2 innate lymphoid cells in the inflamed lung

ED Tait Wojno[1,2,*], **LA Monticelli**[1], **SV Tran**[1], **T Alenghat**[2,**], **LC Osborne**[1], **JJ Thome**[3], **C Willis**[4], **A Budelsky**[4], **DL Farber**[3,5], and **D Artis**[1]

[1]Jill Roberts Institute for Research in Inflammatory Bowel Disease, Joan and Sanford I. Weill Department of Medicine, Weill Cornell Medical College, Cornell University, New York, New York, USA

[2]Institute for Immunology and Department of Microbiology, Perelman School of Medicine, University of Pennsylvania, Philadelphia, Pennsylvania, USA

[3]Columbia Center for Translational Immunology and Department of Microbiology and Immunology, Columbia University Medical Center, New York, New York, USA

[4]Department of Inflammation Research, Amgen Inc., Seattle, Washington, USA

[5]Department of Surgery, Columbia University Medical Center, New York, New York, USA.

Abstract

Group 2 innate lymphoid cells (ILC2s) promote type 2 cytokine-dependent immunity, inflammation and tissue repair. While epithelial cell-derived cytokines regulate ILC2 effector functions, the pathways that control the *in vivo* migration of ILC2s into inflamed tissues remain poorly understood. Here, we provide the first demonstration that expression of the prostaglandin D_2 (PGD_2) receptor CRTH2 (chemoattractant receptor homologous molecule expressed on Th2 cells) regulates the *in vivo* accumulation of ILC2s in the lung. While a significant proportion of ILC2s isolated from healthy human peripheral blood expressed CRTH2, a smaller proportion of ILC2s isolated from non-diseased human lung expressed CRTH2, suggesting that dynamic regulation of CRTH2 expression might be associated with the migration of ILC2s into tissues. Consistent with this, murine ILC2s expressed CRTH2, migrated towards PGD_2 *in vitro* and accumulated in the lung in response to PGD_2 *in vivo*. Further, mice deficient in CRTH2 exhibited reduced ILC2 responses and inflammation in a murine model of helminth-induced pulmonary type 2 inflammation. Critically, adoptive transfer of CRTH2-sufficient ILC2s restored pulmonary inflammation in CRTH2-deficient mice. Together, these data identify a role for the PGD_2-CRTH2

Correspondence: David Artis, PhD, Weill Cornell Medical College, Cornell University, 413 East 69th Street, Belfer Research Building, Room 502 (Box 190), New York, New York, USA; dartis@med.cornell.edu; T: 6469626291.

*Current address: Baker Institute for Animal Health, Department of Microbiology and Immunology, College of Veterinary Medicine, Cornell University, Ithaca, New York, USA.

**Current address: Department of Pediatrics, Cincinnati Children's Hospital, University of Cincinnati, Cincinnati, Ohio, USA.

DISCLOSURE

Cynthia Willis and Alison Budelsky are employees and shareholders of Amgen Inc. The authors have no additional financial interests.

pathway in regulating the *in vivo* accumulation of ILC2s and the development of type 2 inflammation in the lung.

INTRODUCTION

Group 2 innate lymphoid cells (ILC2s) are innate immune cells found in multiple tissues of humans and mice that can promote expulsion of helminth parasites, allergic inflammation, tissue repair and metabolic homeostasis.[1–3] ILC2s in the lung, skin and gut are activated by the predominantly epithelial cell-derived cytokines interleukin (IL)-25, IL-33 and thymic stromal lymphopoietin to produce T helper type 2 (Th2)-associated cytokines such as IL-5, IL-9 and IL-13 and the growth factor amphiregulin.[1,3–7] Despite advances in our understanding of the factors that control the development, activation and effector function of ILC2s, the pathways that regulate their migration into inflamed tissues remain poorly characterized.

In humans, ILC2s have been identified in the peripheral blood, lung, gut, skin and nasal polyps as lineage marker negative (lin^-) cells that express the IL-7 receptor (R)α (CD127) and the IL-33R.[1,3–8] A proportion of human ILC2s also express the prostaglandin D_2 (PGD_2) receptor chemoattractant receptor homologous molecule expressed on Th2 cells (CRTH2).[8–10] In Th2 cells, eosinophils, basophils and mast cells, PGD_2 ligation of CRTH2 causes receptor internalization and downregulation and promotes migration of cells.[11–13] However, while human $CRTH2^+$ ILC2s migrate and produce IL-13 in response to PGD_2 *in vitro*,[14,15] the influence of the PGD_2-CRTH2 pathway on the *in vivo* activation, accumulation and/or effector function of human or murine ILC2s is unknown.

In this report we provide the first demonstration that the PGD_2-CRTH2 pathway promotes the *in vivo* accumulation of ILC2s in the lung in the context of type 2 inflammation. While a significant proportion of ILC2s in the blood of previously healthy adult human organ donors were $CRTH2^+$, a smaller proportion of ILC2s isolated from lung tissue expressed CRTH2, suggesting that the tissue localization of ILC2s and CRTH2 expression may be linked. Consistent with this, the PGD_2-CRTH2 pathway promoted the *in vitro* migration of murine ILC2s and their *in vivo* accumulation in lung tissue. Further, employing a murine model of helminth-induced type 2 pulmonary inflammation, we identify a previously unrecognized role for ILC2-intrinsic expression of CRTH2 in mediating the accumulation of ILC2s in the inflamed lung. Collectively, these findings identify that expression of CRTH2 on ILC2s has a critical role in promoting their accumulation *in vivo* and the development of type 2 inflammation in the lung.

RESULTS

Tissue-specific expression of CRTH2 by human ILC2s

To begin to investigate whether the PGD_2-CRTH2 pathway might be associated with ILC2 responses or accumulation in tissues *in vivo*, we first compared CRTH2 expression on human ILC2s isolated from the peripheral blood versus lung parenchyma from previously healthy deceased adult organ donors at the time of organ procurement for transplantation.

ILC2s were identified using flow cytometry as negative for expression of known cell lineage markers and positive for expression of CD127 and the IL-33R (Figure 1a,b) (see Supplemental Figure 1a,b for staining controls).[8,16] Consistent with previous studies,[8] a significant proportion of ILC2s in peripheral blood mononuclear cells (PBMCs) were $CRTH2^+$ (Figure 1a,c). In contrast, a lower frequency of ILC2s in the lung was $CRTH2^+$ when CRTH2 expression by ILC2s in the PBMCs and lung parenchyma from the same deceased adult organ donor were compared (Figure 1b,c). Given that PGD_2 ligation results in the downregulation of CRTH2 on immune cells,[15,17] these data suggest that CRTH2-expressing ILC2s in the peripheral blood may encounter PGD_2 and downregulate surface CRTH2 expression, associated with their accumulation in the lung.

Murine ILC2s express CRTH2 and accumulate in the lung *in vivo* in response to PGD_2

To experimentally test the role of the PGD_2-CRTH2 pathway in regulating ILC2 responses and accumulation in the lung *in vivo*, we first sought to characterize expression of CRTH2 on murine ILC2s. As there is currently no antibody available to detect murine CRTH2, expression of CRTH2 on murine ILC2s has not been reported previously. Therefore, we employed single cell RNA transcript staining for *Gpr44* (the gene encoding CRTH2) and flow cytometry to assess CRTH2 expression on murine ILC2s from the peripheral blood and lung. Murine ILC2s isolated from PBMCs (see Supplemental Figure 2a for staining controls) expressed *Gpr44* (Figure 2a). Similar to results observed when examining human ILC2s (Figure 1), murine ILC2s isolated from the lung (see Supplemental Figure 2b for staining controls) expressed very low levels of *Gpr44* compared to those in the peripheral blood (Figure 2b), though non-quantitative reverse transcriptase PCR for *Gpr44* on sort-purified murine lung ILC2s confirmed that ILC2s isolated from the murine lung do indeed express this transcript (Figure 2c). These data suggest that expression of CRTH2 and tissue-specific regulation of CRTH2 expression patterns are conserved in human and murine ILC2s.

Previous *in vitro* studies demonstrated that the PGD_2-CRTH2 pathway promotes cytokine production from human ILC2s,[14,15,18] provoking the hypothesis that CRTH2 expression by murine ILC2s may also be associated with cytokine production in response to PGD_2. Following culture of sort-purified murine lung ILC2s with recombinant murine (rm)IL-25, IL-33 and/or PGD_2, rmIL-33 exposure induced robust IL-5, IL-9 and IL-13 production, and rm-IL-25 exposure induced robust IL-5 and IL-13 production from ILC2s (Supplemental Figure 3a,b). However, PGD_2 alone did not elicit cytokine production from murine lung ILC2s and did not significantly augment cytokine production elicited by IL-25 or IL-33 (Supplemental Figure 3a,b). These observations suggest that PGD_2 does not elicit production of effector cytokines from murine lung ILC2s, consistent with their low expression of CRTH2.

The PGD_2-CRTH2 pathway has also been shown to promote chemotaxis of human ILC2s,[14,15] suggesting that CRTH2-expressing murine ILC2s may migrate *in vitro* or accumulate in tissues *in vivo* in response to PGD_2. Using an *in vitro* chemotaxis assay, we observed that sort-purified murine lung ILC2s exhibited limited migration to increasing doses of PGD_2 (Figure 2d). In contrast, murine ILC2s isolated from the spleen migrated

toward PGD_2 more robustly (Figure 2d), and linear regression of the dose-response curves of spleen-derived compared to lung-derived ILC2s to PGD_2 resulted in statistically different best-fit lines (Supplemental Figure 4). These data are consistent with the hypothesis that ILC2s in the periphery could respond to PGD_2 to accumulate in the lung. To directly test whether PGD_2 signaling through CRTH2 promotes accumulation of ILC2s in the lung *in vivo*, wild-type (WT) mice and mice deficient in CRTH2 (*Gpr44*$^{-/-}$ mice) were treated intranasally (i.n.) for 3 days with PGD_2. Following PGD_2 treatment, ILC2s accumulated in the lungs of WT but not *Gpr44*$^{-/-}$ mice (Figure 2e). Together, these data provide the first *in vivo* evidence of a role for the PGD_2-CRTH2 pathway in regulating the migration and/or accumulation of ILC2s in the lung.

Accumulation of ILC2s and type 2 inflammation in the murine lung are dependent on CRTH2

The data shown above, in conjunction with studies showing that ILC2-derived Th2 cytokine-associated responses can contribute to allergic airway inflammation and chronic pulmonary inflammation,[3,7,10,19–21] support the hypothesis that CRTH2 expression may regulate ILC2 accumulation in the context of type 2 cytokine-associated inflammation in the lung. To test this, we employed a murine model of helminth-induced pulmonary type 2 inflammation.[22–25] In this model, larvae of the gastrointestinal nematode *Nippostrongylus brasiliensis* migrate through the lung of mice and elicit severe, pulmonary type 2 inflammation, associated with infiltration of $CD4^+$ T cells and alternatively-activated macrophages and the development of emphysema, which persists long after all helminths are expelled from the intestine.22–25 Following infection with *N. brasiliensis*, WT and *Gpr44*$^{-/-}$ mice had similar numbers of larvae in the lung 50 hours post-infection (p.i.) (Supplementary Figure 5a) and both WT and *Gpr44*$^{-/-}$ mice efficiently cleared parasites from the small intestine by day 10 p.i. (Supplementary Figure 5b), suggesting that CRTH2 deficiency does not significantly impact the lifecycle of *N. brasiliensis* at these time points in the murine host.

However, when helminth-induced accumulation of ILC2s in the inflamed lung was examined at day 32 p.i. in WT and *Gpr44*$^{-/-}$ mice, we observed a helminth-induced increase in the total number of ILC2s in the lung of WT mice but not *Gpr44*$^{-/-}$ mice, as determined using flow cytometry (Figure 3a). Additionally, WT mice exhibited severe histopathological changes (Figure 3b,c), extensive goblet cell hyperplasia (Figure 3d), increased expression of genes associated with type 2 inflammation (*Il4* and *Il13*) (Figure 3e), an increase in the total number of infiltrating cells (Supplemental Figure 6a) and an increase in the total number of $CD4^+$ T cells (Figure 3f) and $CD11b^+CD11c^{int}$ macrophages (Figure 3g) in the lung parenchyma. Remarkably, these responses were significantly diminished in *Gpr44*$^{-/-}$ mice (Figure 3b–g and Supplemental Figure 6a). Notably, the decreased expression of *Il4* and *Il13* in *Gpr44*$^{-/-}$ mice compared to WT mice was not accompanied by changes in expression of IL-17A (Supplemental Figure 6b), and levels of interferon-γ could not be detected in any naïve or infected animals (data not shown). In addition, in agreement with previous findings,[26] expression of *Il5* was not altered in *Gpr44*$^{-/-}$ mice (Supplemental Figure 6c). These analyses suggest that CRTH2 deficiency does not promote the development of a type 1 or type 17 cytokine milieu in the lung

following *N. brasiliensis* infection, but rather selectively regulates expression of specific type 2 cytokines. Together, these data indicate that genetic deletion of CRTH2 is associated with reduced accumulation of ILC2s, less severe pathological changes and decreased expression of *Il4* and *Il13* and immune cell infiltrate in the lung following *N. brasiliensis* infection.

A CRTH2-specific inhibitor limits accumulation of ILC2s and type 2 inflammation in the murine lung following helminth infection

Small molecule inhibitors of CRTH2 have recently been developed,[27] and studies are ongoing to determine whether these drugs could be used to treat allergic disease in humans.[27–29] To complement our studies of mice genetically deficient in *Gpr44*, we sought to determine whether chemical inhibition of CRTH2 using the CRTH2-specific inhibitor OC000459 could also limit helminth-induced accumulation of ILC2s and type 2 inflammation in the lung. Mice infected with *N. brasiliensis* were treated daily with 1 mg/kg OC000459[28] or vehicle, starting 2 days prior to infection, and examined at day 32 p.i. Consistent with our observations in *Gpr44*$^{-/-}$ mice, mice treated with OC000459 had lower total numbers of ILC2s in the lung following infection than control mice treated with vehicle (Figure 4a). In addition, OC000459-treated mice exhibited less severe helminth-induced histopathological changes (Figure 4b,c), decreased expression of *Il4* and *Il13* (Figure 4e) and significantly decreased total numbers of CD4^{+} T cells (Figure 4f) and CD11b^{+}CD11c^{int} macrophages (Figure 4g) in the lung following *N. brasiliensis* infection compared to vehicle-treated control mice. Interestingly, OC000459-treated mice and vehicle-treated controls demonstrated similar goblet cell hyperplasia in the lung following infection (Figure 4d). These data suggest that chemical inhibition of CRTH2, similar to genetic deletion of *Gpr44*, results in reduced accumulation of ILC2s, pathological changes, expression of *Il4* and *Il13* and immune cell infiltrate in the lung following *N. brasiliensis* infection.

Hematopoietic cell expression of CRTH2 is required for accumulation of ILC2s and type 2 inflammation in the murine lung

While CRTH2 expression is enriched in inflammatory cells, non-hematopoietic cells have also been reported to express CRTH2.[11,30,31] To assess the role of hematopoietic cell-intrinsic expression of CRTH2 in promoting ILC2 responses and pulmonary inflammation, lethally irradiated WT mice were reconstituted with congenic WT or *Gpr44*$^{-/-}$ bone marrow (BM) and subjected to the *N. brasiliensis*-induced model of pulmonary type 2 inflammation. WT hosts reconstituted with WT BM (WT-WT BM mice) exhibited significantly increased total numbers of ILC2s (Figure 5a), helminth-induced histopathological changes (Figure 5b,c), goblet cell hyperplasia (Figure 5d), significantly increased expression of *Il4* and *Il13* (Figure 5e) and significantly increased total numbers of CD11b^{+}CD11c^{int} macrophages (Figure 5g) in the lung. In contrast, all of these parameters were reduced in WT hosts reconstituted with *Gpr44*$^{-/-}$ BM (WT-KO BM mice) (Figure 5a–e,g). Notably, WT-WT BM and WT-KO BM mice had similar total numbers of CD4^{+} T cells in the lung following *N. brasiliensis* infection (Figure 5f), suggesting that elevated numbers of CD4^{+} T cells alone do not result in histopathological changes in the lung. These data indicate that hematopoietic CRTH2 expression mediates parameters of helminth-induced pulmonary inflammation in mice.

CRTH2 expression on murine ILC2s promotes their preferential accumulation in the lung and associated type 2 pulmonary inflammation

Next, we assessed the role of ILC2-intrisic CRTH2 expression in regulating the accumulation of ILC2s in the lung by employing mixed BM chimeras in which 50% of donor cells were WT and 50% of donor cells were *Gpr44*$^{-/-}$ (WT-50/50 mice). Following induction of the *N. brasiliensis*-induced model of type 2 inflammation in the lung, the majority of ILC2s present in the lung of infected chimeras were of WT origin (Figure 5h,i), suggesting that ILC2-intrinsic CRTH2 expression is required for efficient accumulation of ILC2s in the lung in a competitive environment. Finally, to test whether CRTH2 expression on ILC2s is sufficient to promote pulmonary inflammation, *Gpr44*-sufficient ILC2s were sort-purified from CD45.1^{+} WT mice (Figure 6a) (see Supplemental Figure 7 for staining controls) and adoptively transferred once weekly into congenic CD45.2^{+} *Gpr44*$^{-/-}$ mice subjected to the *N. brasiliensis*-induced model of type 2 pulmonary inflammation. At day 32 p.i., congenic donor-derived ILC2s could be detected in the lung, retained expression of CD127 and the IL-33R and were capable of producing IL-13 (Figure 6b). These donor-derived ILC2s constituted approximately 5% of the total ILC2 population in the lung of the recipient mice (Supplemental Figure 8). Despite this relatively low frequency, *Gpr44*$^{-/-}$ mice that received these WT ILC2s exhibited increased helminth-induced histopathological changes (Figure 6c,d), increased goblet cell hyperplasia (Figure 6e), elevated expression of *Il4* and *Il13* (Figure 6f) and significantly increased total numbers of CD4^{+} T cells (Figure 6g) and CD11b^{+}CD11c^{int} macrophages (Figure 6h) in the lung parenchyma compared to *Gpr44*$^{-/-}$ mice that did not receive WT ILC2s. Collectively, these data provide evidence that ILC2-intrinsic CRTH2 regulates the accumulation of murine ILC2s in the lung that is associated with ILC2 accumulation, histopathological changes, expression of specific type 2 cytokines and infiltration of immune cells.

DISCUSSION

Previous studies have reported that ILC2s play a critical role in promoting Th2 cytokine-associated inflammation or tissue repair in the lung,[1,3,7,16,19–21] but the factors that influence the *in vivo* migration and accumulation of ILC2s in the lung and other tissues are poorly characterized. By assessing differential expression of CRTH2 by human ILC2s isolated from distinct anatomical compartments, we observed tissue-specific surface expression of CRTH2 that may be associated with ILC2 accumulation in the lung. Studies employing a murine model of type 2 pulmonary inflammation showed that the PGD_2-CRTH2 pathway functions *in vivo* to regulate the accumulation of ILC2s in the murine lung and the development of associated type 2 inflammation. Together, these findings identify a previously unappreciated role for the PGD_2-CRTH2 pathway in regulating the *in vivo* accumulation of ILC2s that supports type 2 cytokine-associated inflammation in the lung.

The observation that there is differential expression of CRTH2 by ILC2s isolated from human or murine peripheral blood and lung could also mean that lung tissue-resident ILC2s and circulating peripheral ILC2s are in fact distinct populations. Additional work is required to carefully dissect how the ILC2 population in the lung is regulated, particularly regarding whether the population expands during inflammation via migration of new cells into the

tissue or by proliferation of tissue-resident cells. Regardless, our data may indicate that there could be heterogeneity within the ILC2 population, which might be determined by anatomical location or following exposure to activating factors. Notably, our data showing that only a small proportion of CRTH2-sufficient ILC2s are needed to drive helminth-induced type 2 inflammation in the lung in CRTH2-deficient mice suggests that this heterogeneity may have profound functional consequences.

Notably, *Gpr44*$^{-/-}$ mice do not display defects in the population size of ILC2s in the lung in the steady-state, suggesting that while CRTH2-dependent pathways promote accumulation of ILC2s in the lung in the context of inflammation, the seeding of ILC2s in the lung during development and in the steady-state does not require CRTH2. These findings indicate that other pathways, including selective expression of chemokine receptors or adhesion molecules, may regulate the recruitment and retention of ILC2s in tissues during development, the steady-state and ongoing inflammation. Further studies will be required to delineate how CRTH2-dependent and -independent pathways differentially regulate the migration of ILC2s in multiple tissues in the context of health and multiple disease states.

ILC2s can interact with a variety of innate and adaptive cell types to orchestrate inflammation.[1,3,7,32] In particular, recent work has focused the role of ILC2s in supporting CD4$^+$ T cell function and accumulation.[33–36] Our data demonstrating that *N. brasiliensis*-induced pulmonary accumulation of CD4$^+$ T cells is dependent on CRTH2-expressing ILC2s (Figure 6g) support these findings. Interestingly however, our studies of chimeric mice show that CD4$^+$ T cell accumulation in the lung following *N. brasiliensis* infection is not dependent on hematopoietic expression of CRTH2 (Figure 5f). Together, these data suggest that the accumulation of CD4$^+$ T cells in this model may be dependent on CRTH2 expression by both ILC2s and non-hematopoietic cells. Alternatively, reconstituted CD4$^+$ T cells in radiation chimeras may be more readily activated than those in normal mice, allowing them to overcome the requirement for CRTH2-expressing ILC2s in mediating their accumulation in the lung. Further studies will be required to understand complex mechanisms that control CD4$^+$ T cell population size in the lung following *N. brasiliensis* infection.

As the accumulation of ILC2s associated with the development of type 2 inflammation in the lung was CRTH2-dependent using genetic deletion of *Gpr44* and chemical inhibition of CRTH2, our studies also support the concept that the PGD_2-CRTH2 pathway may be a viable drug target for the treatment of multiple chronic inflammatory diseases of the airways that are associated with ILC2 responses including allergic rhinitis, asthma and chronic obstructive pulmonary disease (COPD).[3,13,27–29] A number of inhibitors of CRTH2 have already been tested in the treatment of various disease states. Although some studies reported that inhibition of CRTH2 was unsuccessful in ameliorating symptoms of COPD or asthma and allergic rhinitis in patients,[31,37,38] other clinical trials targeting CRTH2 have shown promising efficacy data in the treatment of asthma and allergic rhinitis.[28,39,40] Notably, our results showed that chemical inhibition of CRTH2 ameliorated some, but not all, effects of helminth infection in the lung, as OC000459 treatment did not appear to decrease helminth-induced pulmonary goblet cell hyperplasia. Thus, further trials that include clinically-stratified patient cohorts based on disease activity and assessment of

multiple parameters of disease may be required to determine whether CRTH2 is an appropriate target to treat inflammatory diseases in the lung. Notwithstanding this, our findings are the first to describe a mechanism by which ILC2s accumulate in the lung during inflammation and suggest that the PGD_2-CRTH2-ILC2 pathway could be targeted to treat inflammatory disease states that are associated with CRTH2-expressing ILC2s.

METHODS

Human tissues

PBMCs and lung tissue were obtained from deceased adult organ donors at the time of organ procurement for transplantation through the New York Organ Donor Network (NYODN). All NYODN subjects were 65 years of age or younger, free of chronic infections and cancer and HIV^- and HBV/HCV^-. As donors were deceased at the time of tissue collection, this work does not qualify as “human subjects” as confirmed by the Columbia University IRB. PBMCs were prepared by separating lymphocytes with a Ficoll-Paque (GE Healthcare, Pittsburgh, PA) gradient and lysing remaining red blood cells (RBCs) with ammonium-chloride-potassium (ACK) buffer (Lonza, Basel, Switzerland). Single cell suspensions of lung were prepared by incubating the finely chopped tissue for 1 h with 2 mg/mL collagenase D (Roche, Indianapolis, IN) and 20 μg/mL DNase I (Roche), mashing through a wire mesh sieve and a 70 μm cell strainer, lysing RBCs with ACK buffer (Lonza) and separating lymphocytes with a Ficoll-Paque (GE Healthcare) gradient. For flow cytometric analysis, matched PBMCs and lung from the same deceased adult organ donor were compared.

Mice

Male and female C57BL/6 WT, Thy1.1 C57BL/6 and CD45.1 C57BL/6 mice were purchased from the Jackson Laboratories (Bar Harbor, ME). *Gpr44*$^{-/-}$ mice were provided by Amgen Inc. (Seattle, WA). All mice were used at 8–12 weeks of age, and all experiments used age- and sex-matched controls. All animals were housed in specific pathogen-free conditions at the University of Pennsylvania or Weill Cornell Medical College. WT and *Gpr44*$^{-/-}$ female mice were co-housed, and WT and *Gpr44*$^{-/-}$ male mice shared soiled bedding. All experiments were performed under protocols approved by the University of Pennsylvania or Weill Cornell Medical College Institutional Animal Care and Use Committees.

PBMCs were prepared by separating lymphocytes with a Ficoll-Paque (GE Healthcare) gradient and lysing remaining RBCs with ACK buffer (Lonza). Single cell suspensions of murine spleen were prepared by mashing through a 70 μm cell strainer and lysing RBCs with ACK buffer (Lonza). Single cell suspensions of perfused murine lung tissue (right superior lobe) were prepared by incubating finely chopped tissue for 30 min with 2 mg/mL collagenase D (Roche) and 20 μg/mL DNase I (Roche), mashing through a 70 μm cell strainer, lysing RBCs with ACK buffer (Lonza) and counting total cells.

Type 2 pulmonary inflammation

The *N. brasiliensis* life cycle was maintained as previously described.[41] Mice were infected with 500 L3 *N. brasiliensis* larvae subcutaneously, and analyses were performed at day 32 p.i. Lung larvae were quantified at 50 h p.i. by allowing viable larvae to migrate through agarose in a 37°C water bath, and adult worms in the small intestine were quantified directly from intestinal tissues on day 10 p.i., as described previously.[41] Serum antibody titers for *N. brasiliensis*-specific IgG1 were quantified by ELISA as previously described,[42] and any animals that lacked specific IgG1 were omitted. Mice were treated i.n. with 2.5 mg/kg PGD_2 (Cayman Chemical, Ann Arbor, MI) dissolved in 50 μL 1:10 DMSO in PBS,[43] for 3 days. Untreated mice were treated i.n. with 50 μL vehicle (DMSO) as a control, diluted 1:10 in PBS. Mice were treated intra-peritoneally (i.p.) once daily with 1 mg/kg of the CRTH2-specific inhibitor OC000459 (Cayman Chemical) dissolved in 1:100 DMSO in PBS, starting 2 days prior to infection with *N. brasiliensis* and until analysis at day 32 post-infection. Untreated mice were injected i.p. with vehicle (DMSO) as a control, diluted 1:100 in PBS.

Flow cytometry, single cell RNA transcript staining and cell sorting

Single cell suspensions were incubated with Aqua Live/Dead Fixable Dye (Life Technologies, Grand Island, NY) and fluorochrome-conjugated monoclonal antibodies (mAbs) against mouse CD3 (145-2C11), CD4 (GK1.5), CD5 (53-7.3), CD11b (M1/70), CD11c (N418), CD19 (eBio1D3), CD25 (PC61.5), CD45 (30-F11), CD45.1 (A20), CD45.2 (104), CD127 (A7R34), CD90.1 (HIS51), CD90.2 (53-2.1), IL-33R (DJ8, MD Bioproducts, St. Paul, MN), NK1.1 (PK136) or Siglec-F (E50-2440, BD Biosciences, San Jose, CA), or fluorochrome-conjugated mAbs against human CD3 (OKT3), CD4 (OKT4), CD5 (UCHT2), CD14 (61D3), CD16 (CB16), CD19 (HIB19), CD56 (B159), CD25 (BC96), CD45 (HI30), CD127 (eBioRDR5), CRTH2 (BM16, BD Biosciences), FcεR1α (AER-37) or IL-33R (B4E6, MD Bioproducts) (eBioscience, San Diego, CA, unless specified otherwise). For RNA staining analyses, cells were treated according to manufacturer instructions using a commercially available kit (PrimeFlow™ RNA Assay, eBioscience) and compatible commercially available probes for β*2m* (used as a positive control for RNA staining) and *Gpr44* (eBioscience). For intracellular staining, cells were fixed in 2% paraformaldehyde, permeabilized using BD Perm/Wash buffer (BD Biosciences) according to manufacturer instructions and stained with fluorochrome-conjugated mAbs against mouse IL-5 (TRFK5), IL-9 (RM9A4) and IL-13 (eBio13A) (eBioscience). ILC2s are gated as live, $CD45^+lin^-CD4^-CD90.2^+CD25^+CD127^+IL\text{-}33R^+$ or as live, $\beta 2m^+lin^-CD90.2^+CD127^+IL\text{-}33R^+$ in RNA staining analyses. Samples were run on a 4-laser LSR II (BD Biosciences), and FlowJo 8.7.1 (Tree Star, Inc., Ashland, OR) was used to analyze data. Gates were set using FMO controls with less than 5% background accepted. Analysis and presentation of intracellular cytokine staining distributions were performed using SPICE version 5.1 (National Institute of Allergy and Infectious Diseases, Bethesda, MD), downloaded from http://exon.niaid.nih.gov.[44]

For cell sorting, single cell suspensions were prepared from tissues of female mice that had been treated i.p. for 7 days with 300 ng rmIL-33 (R & D Systems, Minneapolis, MN) or treated 3 times i.p. every other day with 2.5 ng rmIL-7 (R & D Systems) plus 15 μg anti-human IL-7 (M25) (Amgen Inc.). For ILC2s, depletions were performed using biotin-

conjugated mAbs against mouse CD5 (53-7.3), CD19 (eBio1D3) and CD11b (M1/70) (eBioscience) and M-280 streptavidin Dynabeads (Life Technologies) according to manufacturer instructions. Cells were incubated with Aqua Live/Dead Fixable Dye (Life Technologies) and fluorochrome-conjugated mAbs as indicated. $CD45^+CD11b^+SiglecF^+$ eosinophils or $CD45^+lin^-CD4^-CD90^+CD25^+CD127^+IL\text{-}33R^+$ ILC2s were sorted using a 4-laser FACSAria II (BD Biosciences) with a 70 μm nozzle.

BM chimeras and cell transfers

Single cell suspensions from the BM of 8 week-old mice were prepared by flushing the femur and tibia with DMEM (Corning, Corning, NY), lysing RBCs with ACK buffer (Lonza) and depleting T cells using a biotin-conjugated mAb against mouse CD5 (53-7.3) (eBioscience) and M-280 streptavidin Dynabeads (Life Technologies) according to manufacturer instructions. Recipients were lethally irradiated with 1000 CyG using a Nordion Gammacell irradiatior (Ottawa, Canada), anaesthetized with Tribromoethanol (Sigma-Aldrich, St. Louis, MO) administered i.p. and given 4×10^6 donor cells i.v. Sulfamexosone/trimethoprim (Hi-Tech Pharmacal, Amityville, NY) was provided in the drinking water for 2 weeks post-reconstitution, and mice were analyzed at 8–12 weeks post-reconstitution.

Sorted ILC2s from mice treated with rmIL-33 and cultured *in vitro* for 3–7 days with rmIL-2 (10 ng/mL), rmIL-7 (10 ng/mL) and rmIL-33 (30 ng/mL) (eBioscience) were transferred every 7 days to mice infected with *N. brasiliensis*, starting on the day of infection. Mice were anaesthetized with Tribromoethanol administered i.p. and given $1–2 \times 10^5$ cells transferred i.v.

Chemotaxis assays

Sorted spleen or lung ILC2s from mice treated with rmIL-33 were allowed to rest for 2 h at 37°C in media. Media with 0–100 nM of PGD_2 was placed in the bottom chamber of Costar 6.5 mm, 5.0 μm Transwell 24-well plates (Corning), and 5×10^4 ILC2s were placed in the top chamber. Cells were incubated for 90 min at 37°C, and the number of cells that had migrated was quantified using CountBrite Absolute Counting Beads (Life Technologies). Counts were normalized as fold increase over media.

In vitro cultures

Sorted lung ILC2s from mice treated with rmIL-33 or mouse IL-7 complexes were cultured for 48 h in media (DMEM with 10% FBS (Denville Scientific, Metuchen, NJ), 1% L-glutamine (Corning), 1% penicillin/streptomycin (Corning), 25 mM HEPES buffer and 55 μM 2-β-mercaptoethanol (Sigma-Alrich)) with or without 50 ng/mL rmIL-25 (R & D Systems) and/or 30 ng/mL rmIL-33 (R & D Systems) and/or 100 nM PGD_2. Cell-free supernatants were collected for ELISA, and cells were used for intracellular cytokine staining following 4 h culture with 50 ng/mL PMA (Sigma-Aldrich), 500 ng/mL ionomycin (Sigma-Aldrich) and 10 μg/mL BFA (Sigma-Aldrich).

ELISA and real-time PCR

Cytokine levels in cell-free supernatants were assessed using standard sandwich ELISA for IL-5 and IL-13 (eBioscience) or using a commercially available ELISA kit for IL-9 (R & D Systems). For real-time PCR, RNA was isolated from lung tissue using an RNeasy Mini Kit (Qiagen, Valencia, CA) or from sort-purified cells using an RNeasy Micro Kit (Qiagen) according to the manufacturer instructions. RT-PCR or real-time PCR was performed on cDNA generated using a Superscript II reverse transcription kit (Life Technologies) using SYBR green master mix (Applied Biosystems) or Taqman Gene Expression Mastermix (Life Technologies) and commercially available primer sets (Qiagen Quantitect or Life Technologies Taqman primer assays). Samples were run on the ABI 7500 real-time PCR system (Life Technologies). RT-PCR products were run on a 3% agarose gel and visualized using a BioRad Gel Doc 1000 and Quantity One software.

Histology

At necropsy, the left lung lobe was inflated with 4% paraformaldehyde administered through tubing inserted through the trachea and stored in 4% paraformaldehyde. Tissues were then paraffin-embedded, and 5 μm sections were stained with hematoxylin and eosin (H & E) or periodic acid schiff/Alcian blue. Image acquisition was performed using a Nikon Eclipse Ti microscope, a Nikon Digital Sight DS-Fi2 camera and NIS-Elements AT version 4.2 acquisition software (Nikon, Tokyo, Japan). Adobe Photoshop was used to adjust brightness, contrast and color balance (changes were applied to the whole image). Blind scoring was performed by a board-certified veterinary pathologist. Scoring reflects emphysema (1–5) and accumulation of macrophages/multinucleated giant cells (1–5), for an overall maximum score of 10.

Statistical analyses

Results are shown as mean ± sem. Linear regression was used to calculate the best-fit line for chemotaxis in response to a dose curve of PGD_2. Statistical significance was determined using an unpaired two-tailed students *t*-test with Welch's correction if needed, a paired two-tailed students *t*-test for paired observations, or a one-way ANOVA test followed by Bonferroni post-hoc testing. Statistical outliers were identified in normal Gaussian data sets using the extreme studentized deviate (ESD) method, and outliers were uniformly omitted. Results were considered significant at *, $P \leq 0.05$; **, $P \leq 0.01$; ***, $P \leq 0.001$. Statistical analyses were performed using Prism version 4.0a (GraphPad Software, Inc., San Diego, CA).

Supplementary Material

Refer to Web version on PubMed Central for supplementary material.

ACKNOWLEDGEMENTS

We thank members of the Artis laboratory and Dr. Garret Fitzgerald for discussions and critical reading of the manuscript. Research in the Artis lab is supported by the NIH (AI061570, AI095608, AI087990, AI074878, AI095466, AI106697, AI102942 and AI097333 to D.A; T32-AI060516 and F32-AI098365 to E.D.T.W.; T32-AI007532 to L.A.M.; K08-DK093784 to T.A.), the Burroughs Wellcome Fund Investigator in Pathogenesis of Infectious Disease Award to D.A., the Crohn's and Colitis Foundation of America to T.A. and D.A., the Irvington

Institute Edmond J. Safra Postdoctoral Fellowship of the Cancer Research Institute to L.C.O. and the NIAID Mucosal Immunology Studies Team (MIST) consortium (U01-AI095608). Research in the Farber lab is supported by the NIH (F31-AG047003 to J.J.T.). We thank the Matthew J. Ryan Veterinary Hospital Pathology Lab and the Abramson Cancer Center Flow Cytometry and Cell Sorting Resource Laboratory (P30-CA016520). The authors also wish to thank Peggy Just, Castle Funatake and Matt Schifano at eBioscience, Inc. for reagents, support and invaluable technical advice.

REFERENCES

1. Licona-Limon P, Kim LK, Palm NW, Flavell RA. TH2, allergy and group 2 innate lymphoid cells. Nature Immunology. 2013; 14(6):536–542. [PubMed: 23685824]
2. Spits H, et al. Innate lymphoid cells--a proposal for uniform nomenclature. Nature Reviews Immunology. 2013; 13(2):145–149.
3. Kim BS, Wojno ED, Artis D. Innate lymphoid cells and allergic inflammation. Current Opinion in Immunology. 2013; 25(6):738–744. [PubMed: 24001372]
4. Koyasu S, Moro K. Innate Th2-type immune responses and the natural helper cell, a newly identified lymphocyte population. Current Opinion in Allergy and Clinical Immunology. 2011; 11(2):109–114. [PubMed: 21301328]
5. Barlow JL, McKenzie AN. Nuocytes: expanding the innate cell repertoire in type-2 immunity. Journal of Leukocyte Biology. 2011; 90(5):867–874. [PubMed: 21712394]
6. Spits H, Cupedo T. Innate lymphoid cells: emerging insights in development, lineage relationships, and function. Annual Review of Immunology. 2012; 30:647–675.
7. Tait Wojno ED, Artis D. Innate lymphoid cells: balancing immunity, inflammation, and tissue repair in the intestine. Cell Host & Microbe. 2012; 12(4):445–457. [PubMed: 23084914]
8. Mjosberg JM, et al. Human IL-25- and IL-33-responsive type 2 innate lymphoid cells are defined by expression of CRTH2 and CD161. Nature Immunology. 2011; 12(11):1055–1062. [PubMed: 21909091]
9. Kim BS, et al. TSLP elicits IL-33-independent innate lymphoid cell responses to promote skin inflammation. Science Translational Medicine. 2013; 5(170):170ra116.
10. Hams E, et al. IL-25 and type 2 innate lymphoid cells induce pulmonary fibrosis. Proceedings of the National Academy of Sciences of the United States of America. 2014; 111(1):367–372. [PubMed: 24344271]
11. Abe H, et al. Molecular cloning, chromosome mapping and characterization of the mouse CRTH2 gene, a putative member of the leukocyte chemoattractant receptor family. Gene. 1999; 227(1):71–77. [PubMed: 9931443]
12. Hirai H, et al. Prostaglandin D2 selectively induces chemotaxis in T helper type 2 cells, eosinophils, and basophils via seven-transmembrane receptor CRTH2. The Journal of Experimental Medicine. 2001; 193(2):255–261. [PubMed: 11208866]
13. Pettipher R. The roles of the prostaglandin D(2) receptors DP(1) and CRTH2 in promoting allergic responses. British Journal of Pharmacology. 2008; 153(Suppl 1):S191–S199. [PubMed: 17965752]
14. Chang JE, Doherty TA, Baum R, Broide D. Prostaglandin D2 regulates human type 2 innate lymphoid cell chemotaxis. The Journal of Allergy and Clinical Immunology. 2013; 133(3):899–901. [PubMed: 24210841]
15. Xue L, et al. Prostaglandin D activates group 2 innate lymphoid cells through chemoattractant receptor-homologous molecule expressed on T2 cells. The Journal of Allergy and Clinical Immunology. 2013; 133(4):1184–1194. [PubMed: 24388011]
16. Monticelli LA, et al. Innate lymphoid cells promote lung-tissue homeostasis after infection with influenza virus. Nature Immunology. 2011; 12(11):1045–1054. [PubMed: 21946417]
17. Gallant MA, et al. Differential regulation of the signaling and trafficking of the two prostaglandin D2 receptors, prostanoid DP receptor and CRTH2. European Journal of Pharmacology. 2007; 557(2–3):115–123. [PubMed: 17207480]
18. Barnig C, et al. Lipoxin A4 regulates natural killer cell and type 2 innate lymphoid cell activation in asthma. Science Translational Medicine. 2013; 5(174):174ra126.

19. Barlow JL, et al. Innate IL-13-producing nuocytes arise during allergic lung inflammation and contribute to airways hyperreactivity. The Journal of Allergy and Clinical Immunology. 2012; 129(1):191–198. e191–e194. [PubMed: 22079492]
20. Bartemes KR, et al. IL-33-responsive lineage- CD25+ CD44(hi) lymphoid cells mediate innate type 2 immunity and allergic inflammation in the lungs. Journal of Immunology. 2012; 188(3): 1503–1513.
21. Halim TY, Krauss RH, Sun AC, Takei F. Lung natural helper cells are a critical source of Th2 cell-type cytokines in protease allergen-induced airway inflammation. Immunity. 2012; 36(3):451–463. [PubMed: 22425247]
22. Urban JF Jr, et al. The importance of Th2 cytokines in protective immunity to nematodes. Immunological Reviews. 1992; 127:205–220. [PubMed: 1354652]
23. Marsland BJ, Kurrer M, Reissmann R, Harris NL, Kopf M. Nippostrongylus brasiliensis infection leads to the development of emphysema associated with the induction of alternatively activated macrophages. European Journal of Immunology. 2008; 38(2):479–488. [PubMed: 18203142]
24. Reece JJ, et al. Hookworm-induced persistent changes to the immunological environment of the lung. Infection and Immunity. 2008; 76(8):3511–3524. [PubMed: 18505812]
25. Turner JE, et al. IL-9-mediated survival of type 2 innate lymphoid cells promotes damage control in helminth-induced lung inflammation. The Journal of Experimental Medicine. 2013; 210(13): 2951–2965. [PubMed: 24249111]
26. Chevalier E, et al. Cutting edge: chemoattractant receptor-homologous molecule expressed on Th2 cells plays a restricting role on IL-5 production and eosinophil recruitment. Journal of Immunology. 2005; 175(4):2056–2060.
27. Ulven T, Kostenis E. Targeting the prostaglandin D2 receptors DP and CRTH2 for treatment of inflammation. Current Topics in Medicinal Chemistry. 2006; 6(13):1427–1444. [PubMed: 16918458]
28. Barnes N, et al. A randomized, double-blind, placebo-controlled study of the CRTH2 antagonist OC000459 in moderate persistent asthma. Clinical and Experimental Allergy: Journal of the British Society for Allergy and Clinical Immunology. 2012; 42(1):38–48. [PubMed: 21762224]
29. Pettipher R, Whittaker M. Update on the development of antagonists of chemoattractant receptor-homologous molecule expressed on Th2 cells (CRTH2). From lead optimization to clinical proof-of-concept in asthma and allergic rhinitis. Journal of Medicinal Chemistry. 2012; 55(7):2915–2931. [PubMed: 22224640]
30. Chiba T, et al. Prostaglandin D2 induces IL-8 and GM-CSF by bronchial epithelial cells in a CRTH2-independent pathway. International Archives of Allergy and Immunology. 2006; 141(3): 300–307. [PubMed: 16940740]
31. Snell N, Foster M, Vestbo J. Efficacy and safety of AZD1981, a CRTH2 receptor antagonist, in patients with moderate to severe COPD. Respiratory Medicine. 2013; 107(11):1722–1730. [PubMed: 23827726]
32. Monticelli LA, Sonnenberg GF, Artis D. Innate lymphoid cells: critical regulators of allergic inflammation and tissue repair in the lung. Current Opinion in Immunology. 2012; 24(3):284–289. [PubMed: 22521139]
33. Drake LY, Iijima K, Kita H. Group 2 innate lymphoid cells and CD4(+) T cells cooperate to mediate type 2 immune response in mice. Allergy. 2014; 69(10):1300–1307. [PubMed: 24939388]
34. Oliphant CJ, et al. MHCII-Mediated Dialog between Group 2 Innate Lymphoid Cells and CD4(+) T Cells Potentiates Type 2 Immunity and Promotes Parasitic Helminth Expulsion. Immunity. 2014; 41(2):283–295. [PubMed: 25088770]
35. Halim TY, et al. Group 2 innate lymphoid cells are critical for the initiation of adaptive T helper 2 cell-mediated allergic lung inflammation. Immunity. 2014; 40(3):425–435. [PubMed: 24613091]
36. Mirchandani AS, et al. Type 2 innate lymphoid cells drive CD4+ Th2 cell responses. Journal of Immunology. 2014; 192(5):2442–2448.
37. Busse WW, et al. Safety and efficacy of the prostaglandin D2 receptor antagonist AMG 853 in asthmatic patients. The Journal of Allergy and Clinical Immunology. 2013; 131(2):339–345. [PubMed: 23174659]

38. Snell NJ. Discontinued drug projects in the respiratory therapeutic area during 2012. Expert Opinion on Investigational Drugs. 2014; 23(3):411–415. [PubMed: 24490845]

39. Horak F, et al. The CRTH2 antagonist OC000459 reduces nasal and ocular symptoms in allergic subjects exposed to grass pollen, a randomised, placebo-controlled, double-blind trial. Allergy. 2012; 67(12):1572–1579. [PubMed: 23025511]

40. Singh D, et al. Inhibition of the asthmatic allergen challenge response by the CRTH2 antagonist OC000459. The European Respiratory Journal. 2013; 41(1):46–52. [PubMed: 22496329]

41. Camberis M, Le Gros G, Urban J Jr. Animal model of Nippostrongylus brasiliensis and Heligmosomoides polygyrus. Current Protocols in Immunology, edited by John E. Coligan … [et al.]. 2003; Chapter 19(Unit 19):12.

42. Mearns H, et al. Interleukin-4-promoted T helper 2 responses enhance Nippostrongylus brasiliensis-induced pulmonary pathology. Infection and Immunity. 2008; 76(12):5535–5542. [PubMed: 18809669]

43. Spik I, et al. Activation of the prostaglandin D2 receptor DP2/CRTH2 increases allergic inflammation in mouse. Journal of Immunology. 2005; 174(6):3703–3708.

44. Roederer M, Nozzi JL, Nason MC. SPICE: exploration and analysis of post-cytometric complex multivariate datasets. Cytometry Part A: The Journal of the International Society for Analytical Cytology. 2011; 79(2):167–174. [PubMed: 21265010]

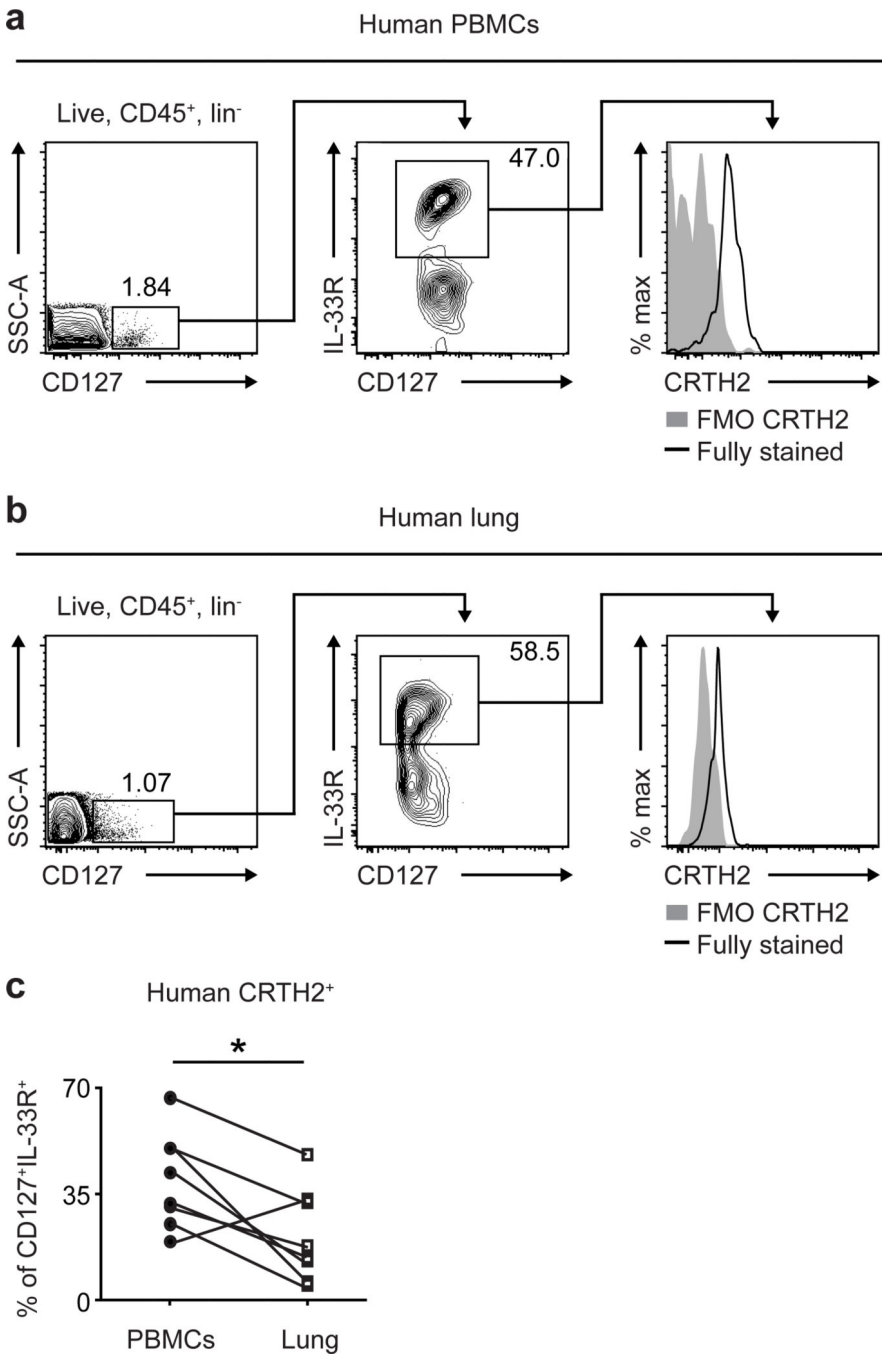

Figure 1. Human ILC2s isolated from the peripheral blood are more likely to express CRTH2 than ILC2s isolated from the lung

CRTH2 expression by CD45$^+$ lineage (CD3/CD5/CD14/CD16/CD19/CD56/FcεRIα) negative (lin$^-$) CD127$^+$IL-33R$^+$ ILC2s in (**a**) PBMCs and (**b**) lung parenchyma from the same deceased adult organ donor (collected at the time of organ procurement for transplantation). Left plots gated on CD45$^+$lin$^-$ cells. FMO, fluorescence minus one negative staining control. (**c**) Frequency of CRTH2$^+$ cells of human CD45$^+$lin$^-$CD127$^+$IL-33R$^+$ ILC2s from the PBMCs and lung parenchyma isolated from the

same deceased adult organ donor. (**a–c**) Blood n=8; lung n=8. Results are mean ± sem; *, $P \leq 0.5$ using (**c**) a paired two-tailed students t-test.

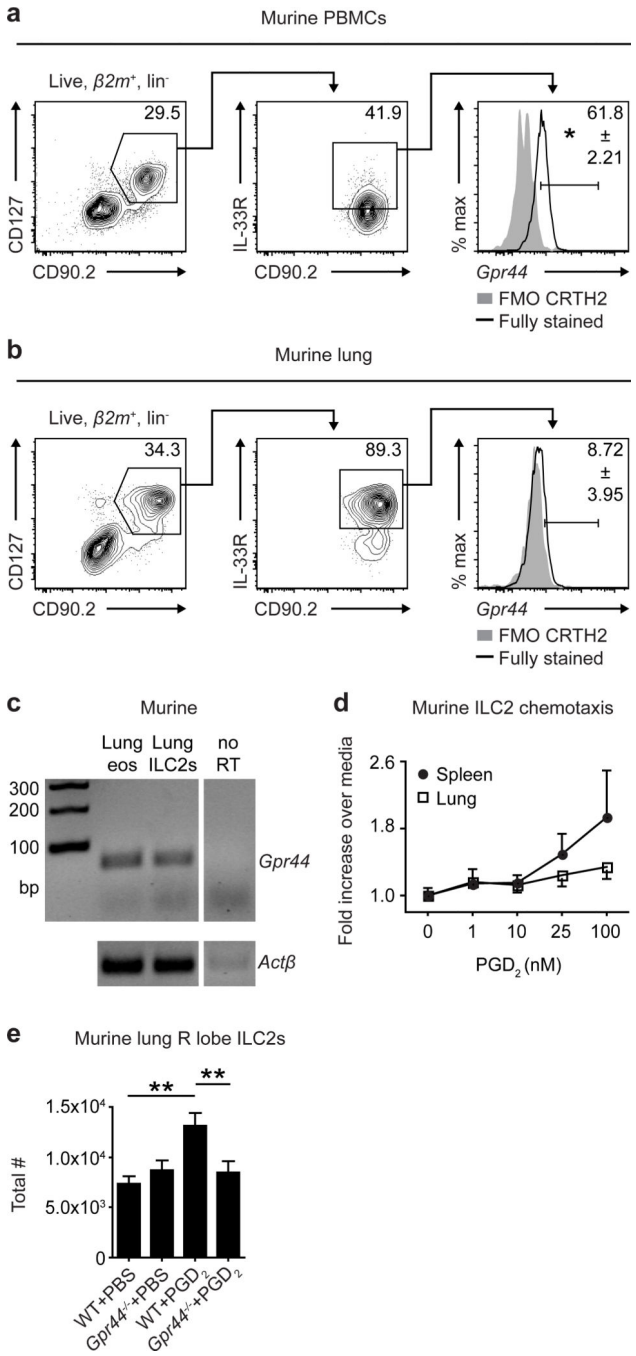

Figure 2. Murine ILC2s express CRTH2 and accumulate in the lung in response to PGD_2

Gpr44 RNA transcript expression by β*2m*$^+$ lineage (CD3/CD4/ CD19/CD11b/CD11c/ NK1.1) negative (lin$^-$) CD90.2$^+$CD127$^+$IL-33R$^+$ ILC2s in (**a**) PBMCs and (**b**) lung parenchyma from C57BL/6 WT mice. Left plots gated on β*2m*$^+$lin$^-$ cells. FMO, fluorescence minus one negative (no probe) staining control. (**c**) *Gpr44* and *Act*β expression in cells sort-purified from rmIL-33-treated C57BL/6 WT mice. As a positive control and consistent with previous studies,[12] lung eosinophils expressed *Gpr44*. (**d**) *In vitro* migration of spleen and lung ILC2s sort-purified from rmIL-33-treated C57BL/6 WT mice in response

to PGD_2. (**e**) Total numbers of ILC2s in the right (R) superior lung lobe of naïve C57BL/6 WT and *Gpr44*$^{-/-}$ mice treated i.n. with PGD_2 for 3 days determined using flow cytometry (ILC2s are $CD45^+$ lineage (CD3/CD4/CD5/CD19/CD11b/CD11c/NK1.1) negative $CD90.2^+CD25^+CD127^+IL\text{-}33R^+$). Data are representative of (**a,b,e**) 2–4 mice per group per experiment and 2 independent experiments or (**c,d**) ILC2s from 5 pooled mice per experiment and 5 independent experiments. Results are mean ± sem; *, $P \leq 0.05$; **, $P \leq 0.01$; using (**a,b**) a two-tailed students *t*-test or (**e**) a one-way ANOVA test and Bonferroni post-hoc testing.

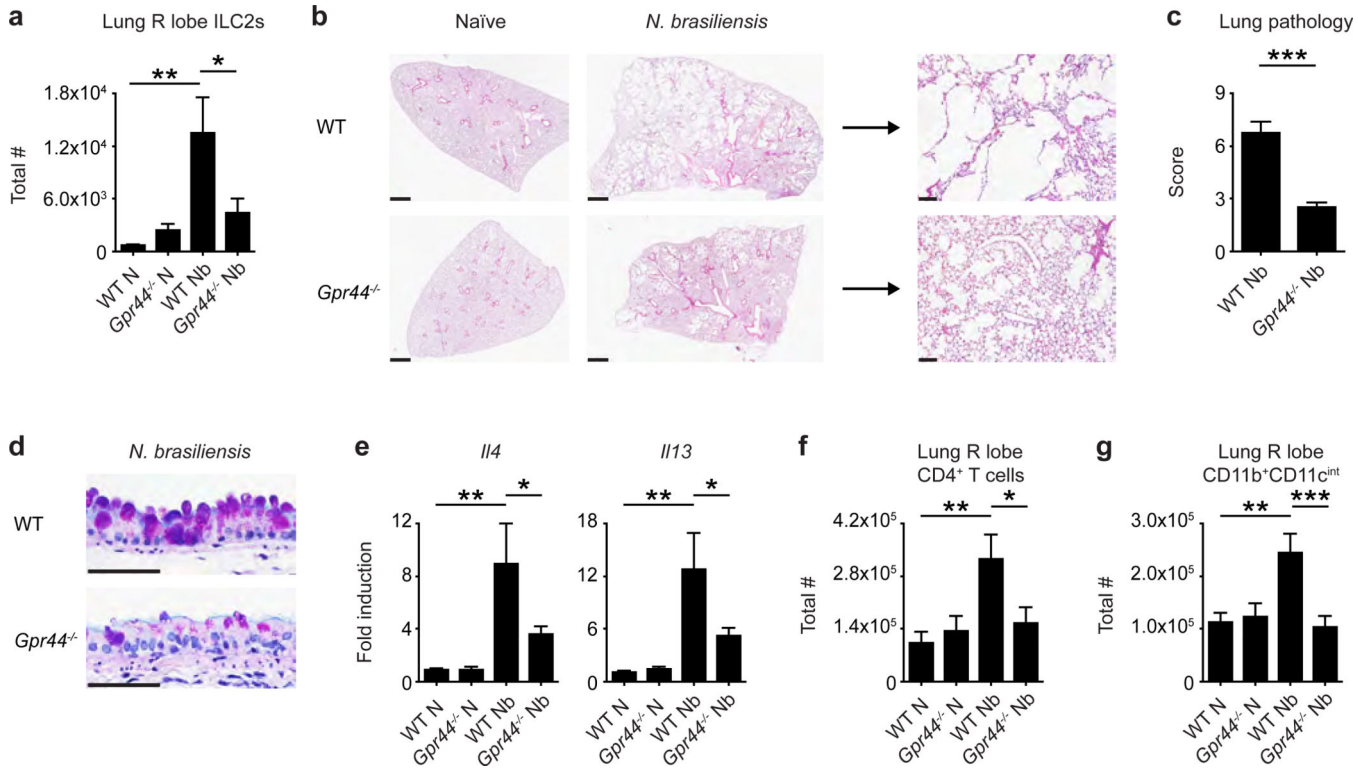

Figure 3. CRTH2 mediates accumulation of ILC2s in the murine lung and pulmonary inflammation

C57BL/6 WT and *Gpr44*$^{-/-}$ mice infected with *N. brasiliensis* were examined at day 32 following infection (N, naive; Nb, *N. brasiliensis*). (**a**) Total numbers of ILC2s in the lung determined using flow cytometry (ILC2s are CD45^{+} lineage (CD3/CD4/CD5/CD19/CD11b/CD11c/NK1.1) negative CD90.2^{+}CD25^{+}CD127^{+}IL-33R^{+}). (**b**) H & E staining of lung sections. Scale bars = 1 mm (left) or 100 μm (right). (**c**) Pathology score based on histology. (**d**) Periodic acid schiff/Alcian Blue staining of lung sections depicting bronchiolar epithelium. Scale bars = 50 μm. (**e**) Real-time PCR analysis of gene expression in lung tissue. Total numbers of (**f**) CD4^{+} T cells and (**g**) CD11b^{+}CD11c^{int} macrophages determined using flow cytometry. Data are representative of 1–4 mice per group per experiment and 5 independent experiments. Results are mean ± sem; *, $P \leq 0.05$; **, $P \leq 0.01$; ***, $P \leq 0.001$ using (**a,e–g**) a one-way ANOVA test and Bonferroni post-hoc testing or (**c**) a two-tailed students *t*-test.

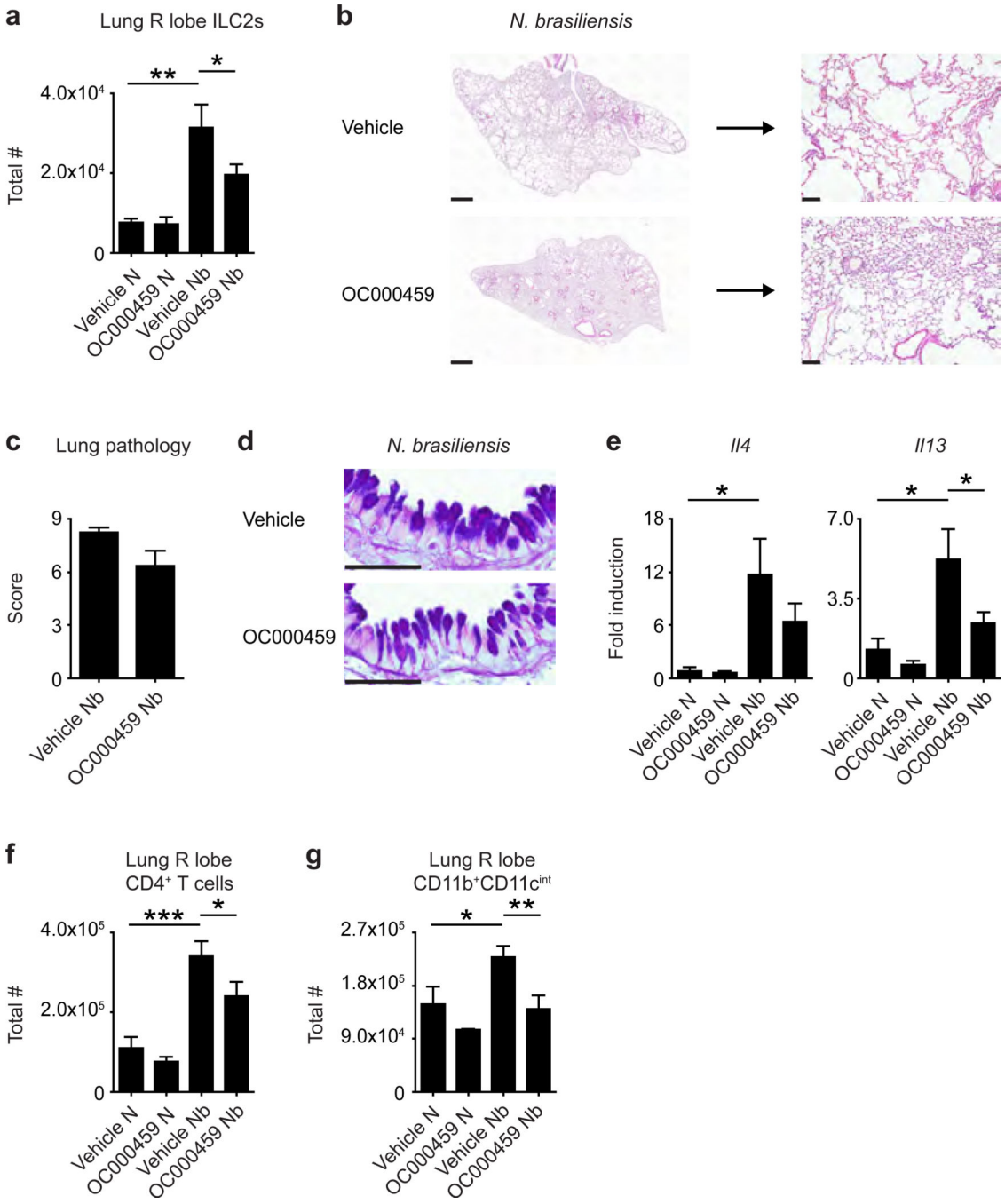

Figure 4. A CRTH2-specific inhibitor prevents accumulation of ILC2s in the murine lung and pulmonary inflammation following helminth infection

C57BL/6 WT mice treated with or without the CRTH2 inhibitor OC00459 infected with *N. brasiliensis* were examined at day 32 following infection (N, naive; Nb, *N. brasiliensis*). (**a**) Total numbers of ILC2s in the lung determined using flow cytometry (ILC2s are $CD45^+$ lineage (CD3/CD4/CD5/CD19/CD11b/CD11c/NK1.1) negative $CD90.2^+CD25^+CD127^+IL\text{-}33R^+$). (**b**) H & E staining of lung sections. Scale bars = 1 mm (left) or 100 μm (right). (**c**) Pathology score based on histology. (**d**) Periodic acid schiff/

Alcian Blue staining of lung sections depicting bronchiolar epithelium. Scale bars = 50 μm. (**e**) Real-time PCR analysis of gene expression in lung tissue. Total numbers of (**f**) $CD4^+$ T cells and (**g**) $CD11b^+CD11c^{int}$ macrophages determined using flow cytometry. Data are representative of 2–4 mice per group per experiment and 2 independent experiments. Results are mean ± sem; *, $P \leq 0.05$; **, $P \leq 0.01$; ***, $P \leq 0.001$ using (**a,e–g**) a one-way ANOVA test and Bonferroni post-hoc testing or (**c**) a two-tailed students *t*-test.

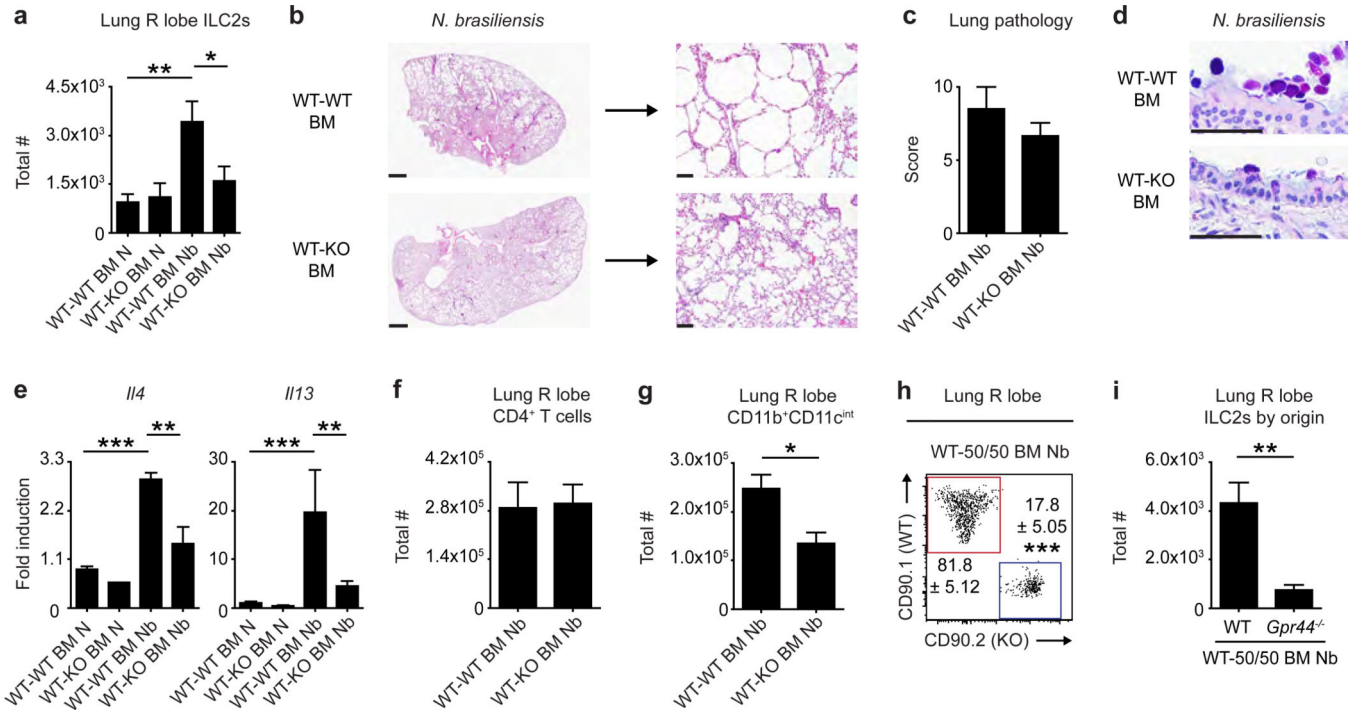

Figure 5. Hematopoietic expression of CRTH2 mediates ILC2 accumulation in the murine lung and pulmonary inflammation

CD45.1 C57BL/6 WT mice were lethally irradiated and reconstituted with CD45.2 C57BL/6 WT bone marrow (BM) (WT-WT BM mice), *Gpr44*$^{-/-}$ BM (WT-KO BM mice) or WT and *Gpr44*$^{-/-}$ BM at a 1:1 ratio (WT-50/50 BM mice). Chimeric mice were infected with *N. brasiliensis* and examined at day 32 following infection (N, naive; Nb, *N. brasiliensis*). (**a**) Total numbers of ILC2s in the lung determined using flow cytometry (ILC2s are CD45.2^{+} lineage (CD3/CD4/CD5/CD19/CD11b/ CD11c/NK1.1) negative (lin^{-}) CD90.2^{+}CD25^{+} CD127^{+} IL-33R^{+}). (**b**) H & E staining of lung sections. Scale bars = 1 mm (left) or 100 μm (right). (**c**) Pathology score based on histology. (**d**) Periodic acid schiff/Alcian Blue staining of lung sections depicting bronchiolar epithelium. Scale bars = 50 μm. (**e**) Real-time PCR analysis of gene expression in lung tissue. Total numbers of (**f**) CD4^{+} T cells and (**g**) CD11b^{+}CD11c^{int} macrophages as determined using flow cytometry. (**h**) Representative flow cytometry plot showing the distribution of donor WT (red) and *Gpr44*$^{-/-}$ (blue) ILC2s (% of ILC2s) and (**i**) total numbers of donor ILC2s of WT and *Gpr44*$^{-/-}$ origin in the lung. Plot gated on CD45.2^{+}lin^{-}CD25^{+}CD127^{+}IL-33R^{+} ILC2s. Data are representative of 2–4 mice per group per experiment and 3 independent experiments. Results are mean ± sem; *, $P \leq 0.05$; **, $P \leq 0.01$; ***, $P \leq 0.001$ using (**a,e**) a one-way ANOVA test and Bonferroni post-hoc testing or (**c,f–i**) a two-tailed students *t*-test and (**i**) Welch's correction for unequal variance.

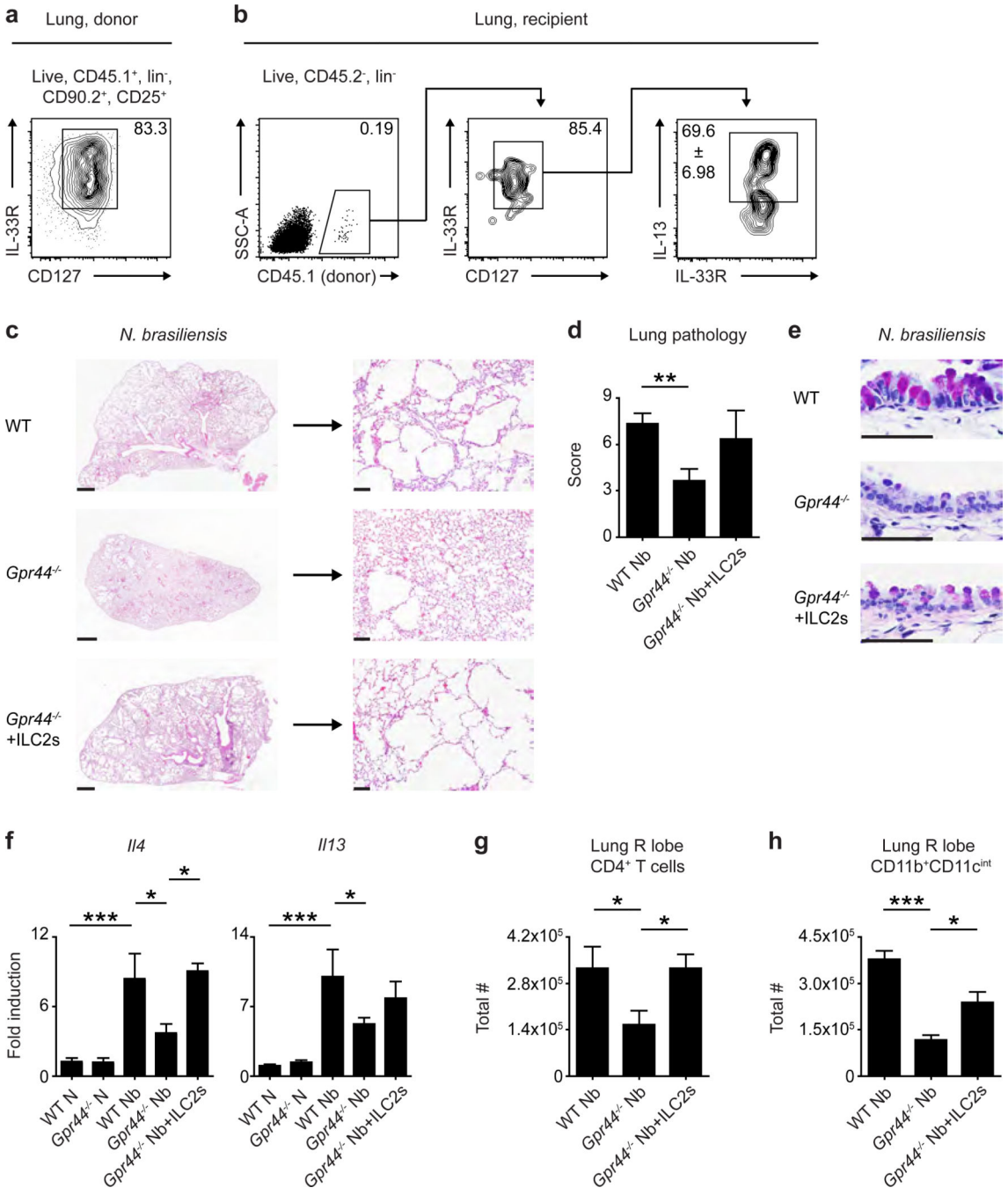

Figure 6. CRTH2-expressing ILC2s mediate pulmonary inflammation in *Gpr44*$^{-/-}$ mice

C57BL/6 WT and *Gpr44*$^{-/-}$ mice infected with *N. brasiliensis* were examined at day 32 following infection (N, naive; Nb, *N. brasiliensis*). Some *Gpr44*$^{-/-}$ mice received pulmonary CD45.1^{+} *Gpr44*$^{+/+}$ ILC2s intra-venously (i.v.) every week starting the day of infection. (**a**) Representative flow cytometry plot showing sort-purified donor CD45.1^{+} *Gpr44*-sufficient ILC2s. Plot gated on CD45.1^{+} lineage (CD3/CD4/CD5/CD19/CD11b/CD11c/NK1.1) negative (lin^{-}) CD90.2^{+}CD25^{+} cells, and percentage is ILC2s of CD45.1^{+} cells. (**b**) Representative flow cytometry plots showing donor CD45.1^{+} *Gpr44*-sufficient

ILC2s in the lung of recipient *Gpr44*$^{-/-}$ mice at day 32 following *N. brasiliensis* infection. Left: gated on CD45.2^{-}lin^{-} cells; middle: gated on CD45.2^{-}lin^{-}CD45.1^{+}CD90.2^{+}CD25^{+} cells; right: gated on donor-derived ILC2s. (**c**) H & E staining of lung sections. Scale bars = 1 mm (left) or 100 μm (right). (**d**) Pathology score based on histology. (**e**) Periodic acid schiff/Alcian Blue staining of lung sections depicting bronchiolar epithelium. Scale bars = 50 μm. (**f**) Real-time PCR analysis of gene expression in lung tissue. Total numbers of (**g**) CD4^{+} T cells and (**h**) CD11b^{+}CD11c^{int} macrophages as determined using flow cytometry. Data are representative of 2–4 mice per group per experiment and 3 independent experiments. Results are mean ± sem; *, $P \leq 0.05$; ***, $P \leq 0.001$ using (**d,f–h**) a one-way ANOVA test and Bonferroni post-hoc testing.